ACS Pharmacology & Translational Science

pubs.acs.org/ptsci

Article

Exploring the Cytotoxic Effects of the Extracts and Bioactive Triterpenoids from *Dillenia indica* against Oral Squamous Cell Carcinoma: A Scientific Interpretation and Validation of Indigenous Knowledge

Maniyamma Aswathy,[#] Kishore Banik,[#] Dey Parama,[#] Parameswaran Sasikumar, Choudhary Harsha, Anuja Gracy Joseph, Daisy R. Sherin, Manojkumar K. Thanathu, Ajaikumar B. Kunnumakkara,* and Radhakrishnan Kokkuvayil Vasu*

Cite This: *ACS Pharmacol. Transl. Sci.* 2021, 4, 834−847

Read Online

ACCESS | Metrics & More | Article Recommendations | Supporting Information

ABSTRACT: Triterpenoids are ubiquitously distributed secondary metabolites, primarily scrutinized as a source of medication and preventive measures for various chronic diseases. The ease of isolation and excellent pharmacological properties of triterpenoids are notable reasons behind the exponential rise of extensive research on the bioactive triterpenoids over the past few decades. Herein, we attempted to explore the anticancer potential of the fruit extract of the ethnomedicinal plant *Dillenia indica* against oral squamous cell carcinoma (OSCC) and have exclusively attributed the efficacy of the extracts to the presence of two triterpenoids, namely, betulinic acid (BA) and koetjapic acid (KA). Preliminary *in vitro* screening of both BA and KA unveiled that the entities could impart cytotoxicity and induce apoptosis in OSCC cell lines, which were further well-supported by virtual screening based on ligand binding affinity and molecular dynamic simulations. Additionally, the aforementioned metabolites could significantly modulate the critical players such as Akt/mTOR, NF-κB, and JAK/STAT3 signaling pathways involved in the regulation of important hallmarks of cancer like cell survival, proliferation, invasion, angiogenesis, and metastasis. The present findings provide insight and immense scientific support and integrity to a piece of indigenous knowledge. However, *in vivo* validation is a requisite for moving to clinical trials and developing it as a commercial drug.

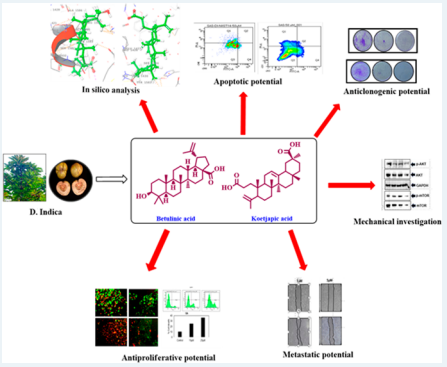

KEYWORDS: *Dillenia indica, triterpenoids, OSCC, cytotoxicity*

Cancer is one of the leading causes of death worldwide, and according to GLOBOCAN 2018, it accounted for approximately 18.1 million new cases and around 9.6 million deaths globally in the year 2018. Oral cancer, or its predominant form, oral squamous cell carcinoma (OSCC), is a major cause of morbidity and mortality in India. It is one of the most aggressive malignancies occurring globally, affecting approximately 354 864 people every year and causing 177384 deaths per year.[1−12] Due to its extremely high recurrence rate, the survival rate percentage of oral cancer patients is one of the lowest among all cancer types. Lifestyle factors like chewing tobacco, areca nut, consumption of alcohol, smoking, high intake of red meat, and fermented food are major risk factors of oral cancer and are the prime reason for its high prevalence.[2,13−16] Despite the significant advancement in the diagnosis and treatment of disease, the incidence of oral cancer is rising quickly due to the lack of sensitive diagnostic methods and effective drugs. The conventional treatment modalities of oral cancer, i.e., surgery, radiation therapy (external beam radiotherapy and/or brachytherapy), and chemotherapy, face numerous limitations such as adverse side effects, high treatment cost, toxicity to healthy cells, chemoresistance, radio resistance, recurrence of the tumor, and so on.[2,3,9,12,17] Thus, there has been a growing interest in developing nontoxic and cost-effective treatments for oral cancer, which comprise complementary and alternative therapies. Exploring natural products and their active components, which exhibit significant chemopreventive and chemotherapeutic potential, has been an area of great attraction for researchers all over the world for the last few decades.[18−25]

Dillenia indica (DI), commonly known as elephant apple, belonging to the family Dilleneaceae, is typically found in the

Received: January 7, 2021
Published: March 9, 2021

https://dx.doi.org/10.1021/acsptsci.1c00011
ACS Pharmacol. Transl. Sci. 2021, 4, 834−847

Scheme 1. Triterpenoids from DI Promotes Apoptosis and Inhibits Metastasis

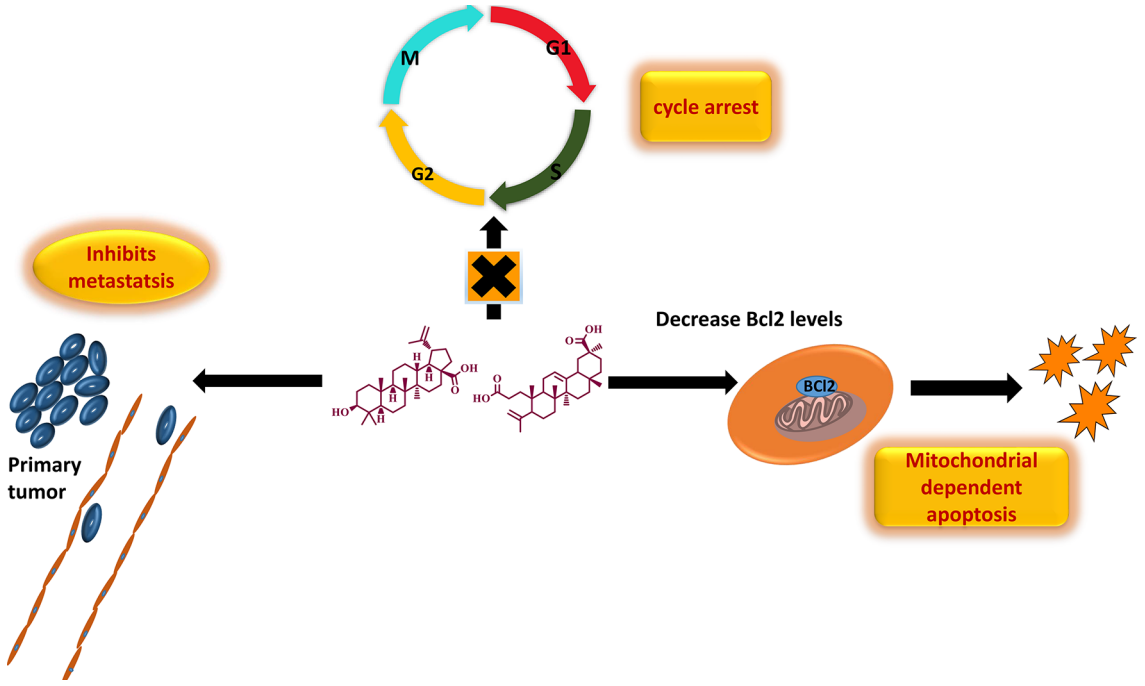

moist forests of the sub-Himalayan region in northeastern India.[26] Fruits of the plant are widely used as a traditional medicine among the tribal population of Mizoram for the treatment of mouth ulcer, diarrhea, and jaundice.[26,27] In addition to this, it is a common culinary ingredient in Assam and is used for preparing jams, pickles, and curries. Besides, the extracts of leaves, fruits, and bark are found to possess medicinal properties and thus are given orally to treat diabetes, cancer, and stomach disorders in the tribal areas of northeastern India.[28,29] The leaves and bark extracts possess antioxidant potential and are also used as a laxative and an astringent agent.[30−34] A thorough investigation of the plant chemistry revealed that it was enriched with triterpenoids, especially the pentacyclic triterpenoids belonging to the lupane group.[35−37] Betulinic acid (BA), a naturally abundant triterpenoid isolated from DI, is reputed as a cytotoxic agent against various malignant tumors.[38−42] Because of its incredible antitumor potential and nontoxic nature towards normal cells, it was established as an excellent cytotoxic agent in a number of cancer cell lines and entered in preclinical trial 1 phase.

Herein, we documented a scientific validation of indigenous knowledge of DI, and identified novel, safe, cost-effective, and multi-targeted anticancer agents from its fruit extract against OSCC. In addition to this, we also identified the bioactive molecules in the species conferring to the corresponding activity via preliminary cytotoxicity assays and *in silico* screening methods. Two of the identified candidates, viz., BA and KA, belong to the class of pentacyclic triterpenoids (Scheme 1). Even though BA is explored as an anticancer agent against numerous malignant tumors, limited reports are available on its potential against OSCC.[43,44] To the best of our knowledge, this is the first report on the anticancer potential of KA against OSCC. The anticancer activity of the identified entities was evaluated using various *in vitro* assays such as 3-[4,5-dimethylthiazol-2-yl]-2,5-diphenyltetrazolium (MTT) assay, clonogenic assay, wound healing assay, fluorescent assisted cell sorting (FACS) analysis, and live and dead assay. Further, Western blot analysis revealed that treatment with DI extracts and compounds significantly modulated multiple signaling pathways such as Akt/mTOR, NF-κB, and JAK/STAT3, thereby exerting anticancer potential.

RESULT AND DISCUSSION

Extraction Strategy and Isolation Procedure of BA and KA. Initially, the sequential extraction of the fruits of *Dillenia indica* Linn. (900 g) were carried out with methanol (2.5 L) as well as water (500 mL) for 3 days; 45 g of methanol extract (DI-ME Ext) and 11 g of aqueous extract (DI-H_2O Ext) were obtained. As a part of our attempt to validate the integrity of the known medicinal properties popularized among the tribal communities, such as the potential of the fruit of DI to cure mouth ulcers and sores, we first analyzed the antiproliferative potential of the fruit extracts through MTT assay against an oral cancer cell line, SAS. The MTT cell proliferation assay is known to assess the metabolic activity of the cells. The amount of insoluble violet-blue formazan produced via the reduction of MTT tetrazolium salt by mitochondrial dehydrogenases determines the percentage of live cells. In this assay, SAS cells treated with an increasing concentration of DI showed reduced growth and proliferation rates of tumor cells, with IC_{50} values of 14 and 12 μg/mL for DI-H_2O Ext and DI-ME Ext respectively (Figure S1).

Because of our keen interest in divulging the phytochemicals in the species which has conferred to the corresponding pharmacological activity, isolation of molecules from DI-ME Ext was performed. For this purpose, DI-ME Ext was preferred over DI-H_2O Ext owing to its lower IC_{50} value. The isolation procedure involved different chromatographic separation techniques, including thin-layer chromatography (TLC), column chromatography (CC) over silica gel (100−200 and 230−400 mesh), sephadex LH 20, and precipitation methods (Figure S2). Surprisingly, two among the ten isolated molecules showed immense cytotoxicity against SAS cell line

https://dx.doi.org/10.1021/acsptsci.1c00011
ACS Pharmacol. Transl. Sci. 2021, 4, 834−847

(Figure S3). Both these molecules belong to the category of triterpenoids: BA, [(3β)-3-hydroxy-lup-20(29)-en-28-oic acid], a pentacyclic triterpenoid is reputed as a cytotoxic agent in various malignant tumor cells and KA is a *seco-A*-ring oleanane group triterpenoid, hitherto uninvestigated from the species, however, reported from the same genus.[45] Characterization was done with sophisticated NMR techniques (^{1}H and ^{13}C) (Tables S1−S10), and structures of the identified bioactive molecules are represented in Figure 1.

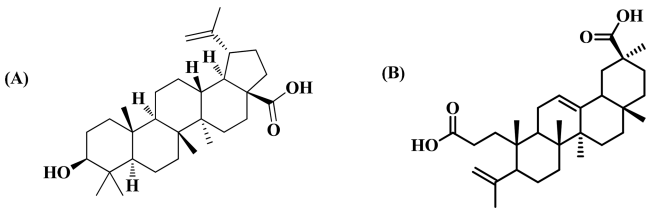

Figure 1. Chemical structures of bioactive molecules (A) BA and (B) KA isolated from DI-ME Ext.

The selection strategy of the entities made by preliminary antiproliferative assay, wherein BA and KA inhibited proliferation at IC_{50} values of 6 and 20 μM respectively after 72 h of treatment (Figure S4).

Computational Screening of BA and KA. Next, the screening strategy was further extended to computational simulation tools, where we employed the molecular docking approach to predict the affinity of the previously screened molecules to bind with the selected protein domains involved in regulating the different hallmarks of cancer (Table S11). Moreover, the flexibility and suitability of the molecules inside the binding pocket of the selected receptors were screened by molecular dynamics protocol.

Molecular Docking. BA was docked against the selected proteins: Akt (Protein Data Bank (PDB) ID: 1O6L), p-Akt, mTOR (PDB ID: 4JSP), p-mTOR, MMP-2 (PDB ID: 3AYU), and VEGF-A (PDB ID: 1FLT) (Table S1). It was found that BA showed a better binding affinity with Akt (D/G-score, −7.5 kcal/mol) and mTOR (D/G-score, −8.4 kcal/mol) (Table 1). In the case of 1O6L, the carboxylate group from the ligand forms H-bonds with polar Thr162 (1.8 and 2.1 Å), while with 4JSP, the carboxylate ion forms a salt bridge with positively charged Lys1452. The salt bridge formation is comparatively stronger and in this case, the ligand is deeply buried inside the binding pocket, thus resulting in maximum binding affinity with 4JSP (Figure 2). Subsequently, KA was docked against NF-κB (1SVC), p-NF-κB, mTOR (4JSP), p-mTOR, STAT3 (6NJS), p-STAT3, CXCR4 (3ODU), COX-2 (5IKQ), survivin (1E31), MMP-2 (1HOV), and VEGF-A (1FLT) (Table 1). Among these, KA showed a better binding affinity with NF-κB (D/G-score, −7.4 kcal/mol), mTOR (D/G-score, −8.1 kcal/mol), and STAT3 (D/G-score, −6.9 kcal/mol) (Table 1). In the binding pocket of 1SVC, one of the carboxylate ions forms H-bonds with positively charged Lys149 (1.9 and 2.2 Å). With 6NJS, one of the carboxylates forms two salt bridges with positively charged Lys573, Lys574, and one H-bond with Lys574 (2.1 Å), and the other carboxylate ion forms H-bond with Asn567 (2.2 Å). Even though two salt bridges are formed with 6NJS, the positioning of the conformer within the binding pocket is not as deep as in the other two cases, which leads to the comparatively lower score with 6NJS. One of the carboxylate ions from KA forms an H-bond with polar Asn1421 (1.8 Å), while the second carboxylate group forms a salt bridge with positively charged Arg2217, eventually contributing to the maximum affinity with 4JSP (Figure 2). The interaction analysis figured out the stability of the ligands inside the binding pocket of the receptor, which is somewhat more in BA as it is well inside the site.

Molecular Dynamics. To visualize the suitability and stability of the ligands inside the binding pocket of the receptor, molecular dynamics simulations were carried out for the complexes 4JSP−BA and 4JSP−KA for 10 000 ps under the OPLS-2005 force field. The RMSD plots (Figure 3) clearly depicts the stability of the complex. Even though the protein shows an initial fluctuation, it is almost stable under 4 Å during the interaction with the BA and KA, whereas the ligands are stabilized inside the protein throughout the trajectory. 4JSP−BA is comparatively more stable with less root-mean-square fluctuations. The P−L histograms (Figure 4) show that the H-bonded interactions are the major force of attraction that holds the ligands inside the protein. The simulation event analysis pointed out the H-bond formation of carboxylate ion of BA with positively charged Lys1452, which lasts for 45% of the simulation time, while that with polar Ser1584 lasts for 49% of the simulation time. However, carboxylate ions of KA form H-bond with positive charged Arg2217 (81 and 96%), hydrophobic Tyr1587 (35%), and polar Ser1584 (52%). Some of the KA residues also form water bridges with both of them. All these factors together subsidize the higher binding affinity of the ligands with mTOR. After evaluating the primary screening based on cancer cell-specific cytotoxicity, followed by molecular docking analysis, the selected candidates were subjected to the next-level studies.

DI Inhibited the Clonogenic Ability of OSCC Cells. We further confirmed the effect of DI on the ability of the individual SAS cells to form colonies by clonogenic assay. Compared with the control, the administration of DI extracts at two different concentrations (10 and 15 μg/mL) caused a significant reduction in the number of colonies. Besides, the treatment of SAS cells with 10 and 15 μM concentrations of both BA and KA was able to reduce the number of colonies in

Table 1. D-Score Values and Residues of BA and KA Interacting with Selected Proteins

	Akt (1O6L)		mTOR (4JSP)	
	D-score (kcal/mol)	interacting residues	D-score (kcal/mol)	interacting residues
BA	−7.5	Thr162	−8.4	Lysl452

	NF-kB (1SVC)		mTOR (4JSP)		STAT3 (6NJS)	
	D-score (kcal/mol)	interacting residues	D-score (kcal/mol)	interacting residues	D-score (kcal/mol)	interacting residues
KA	−7.4	Lysl49	−8.1	Arg2217 Asnl421	−6.9	Lys573 Lys574 Asn567

https://dx.doi.org/10.1021/acsptsci.1c00011
ACS Pharmacol. Transl. Sci. 2021, 4, 834−847

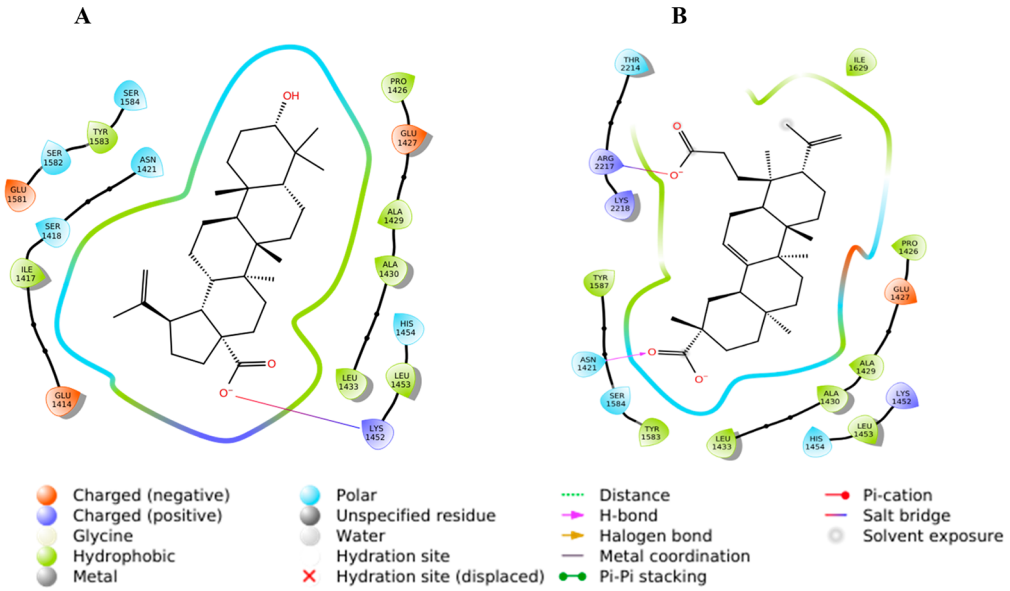

Figure 2. 2D interaction diagrams of (A) BA and (B) KA.

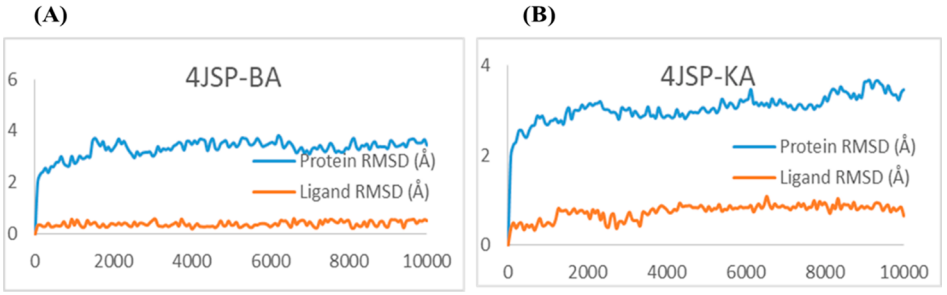

Figure 3. RMSD plots of (A) 4JSP−BA and (B) 4JSP−KA.

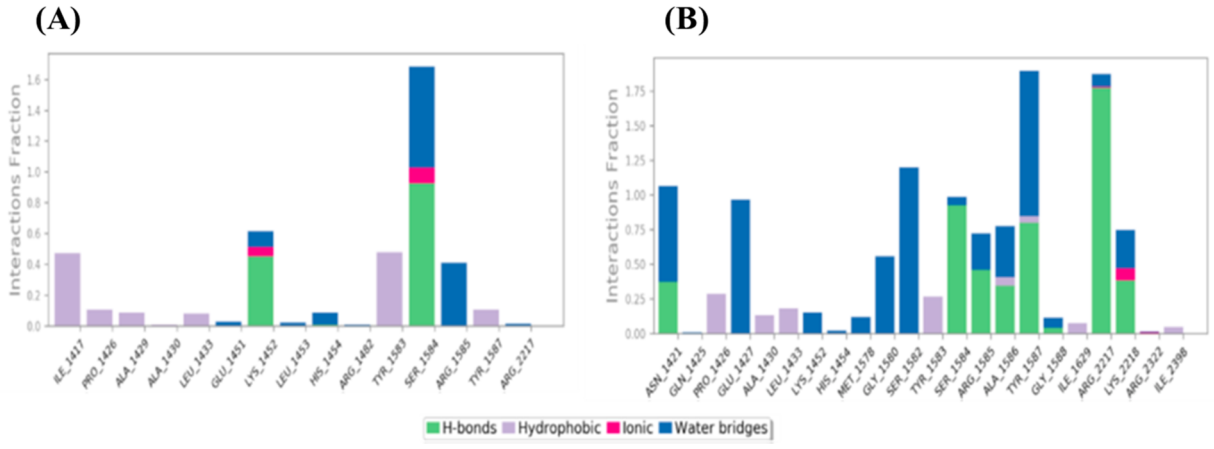

Figure 4. P−L interaction histogram of (A) 4JSP−BA and (B) 4JSP−KA

a dose-dependent manner (Figure 5). In accordance with the clonogenic assay result, it was inferred that KA was superior to BA for inhibiting the colony-forming ability of SAS cells.

DI Induced Cell Death in OSCC Cells. In order to confirm the role of DI in inducing cell death, propidium iodide (PI)-FACS staining was conducted following the treatment of SAS cells with 10 and 20 μg/mL concentrations of both the extracts. Flow cytometric results revealed that the percentage of cell death increased from 14 to 19% in SAS cells treated with DI-H_2O Ext and from 8 to 10% in SAS cells treated with DI-ME Ext after 72 h compared with the untreated control. A similar strategy was followed for elucidating the death inducing potential of BA and KA. Our results showed that BA increased the percentage of cell death from 25% at 10 μM to 36% at 25 μM, whereas KA increased the percentage of cell death from 20% at 25 μM to 33% at 50 μM, respectively (Figure 6(1)). Similarly, in the live and dead assay, treatment with DI led to a dose-dependent toxic effect on OSCC cells. Therefore, the results stated that treatment with the extracts, BA and KA resulted in cell death in SAS cells in a dose-dependent manner.

https://dx.doi.org/10.1021/acsptsci.1c00011
ACS Pharmacol. Transl. Sci. 2021, 4, 834−847

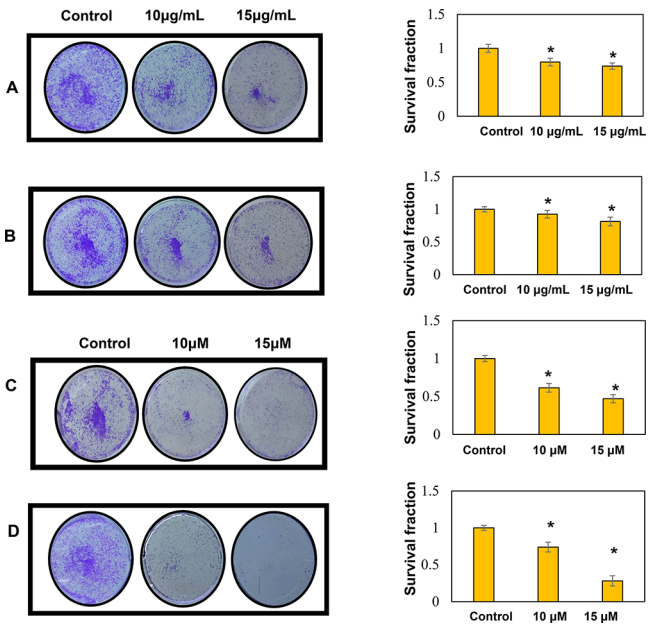

Figure 5. Inhibition of clonogenic potential of SAS cells by (A) DI-H_2O Ext (B) DI-ME Ext (C) BA (D) KA. Untreated cells were kept as the control. Quantification of the number of colonies was done with the help of ImageJ software. Results presented are mean ± SD of three independent experiments; *, $p < 0.05$ vs control.

Effect of DI in Inducing Apoptosis in SAS Cells. Next, we evaluated the potential of DI in inducing apoptosis in SAS cells using Annexin V assay. SAS cells were treated with 10 and 25 μg/mL of DI-H_2O Ext and 25 and 50 μg/mL of DI-ME Ext for 72 h individually. As shown in Figure 7, the percentage of apoptotic cells increased from 1.7% in control to 19.8% under DI-H_2O Ext treatment and from 1% in control to 9% under DI-ME Ext treatment. The percentage of apoptotic cells increased from 3.2% in control to 14.3% in 50 μM BA-treated SAS cells and from 3.2% in control to 12.6% in 50 μM KA-treated SAS cells respectively (Figure 7). These results indicate that BA treatment causes a statistically evident increase in the number of apoptotic cells thus leading to significant growth inhibition in SAS cells.

DI Induced Cell Cycle Arrest in OSCC Cells. To further examine the mechanism of action of DI on SAS cells, the cell cycle distribution was investigated by flow cytometry analysis. We found that the cells upon treatment with different concentrations of DI-H_2O Ext, DI-ME Ext, BA, and KA showed cell cycle arrest at different phases in comparison to the untreated cells. The SAS cells treated with DI-H_2O Ext and DI-ME Ext exhibited G1 and G2 phase arrest, respectively, while BA and KA treated SAS cells demonstrated S phase arrest. This result indicates that the decrease in cell proliferation and viability of the DI-treated SAS cells may be due to the induction of cell cycle arrest at various phases of the cell cycle (Figure 8).

DI Inhibited the Migration of OSCC Cells. The wound healing analysis of SAS cells showed inhibition in the migration of these cells with an increase in the concentration of DI. The images taken at 12 hr in case of DI-H_2O Ext and DI-ME Ext, or 24 hr in case of BA and KA showed that the wound area was completely healed while the treated cells exhibited changes in cell morphology and a significant reduction in the migration of SAS cells compared to the untreated cells. These results indicate that DI controls the migration of SAS cells (Figure 9).

DI Modulated the Expression of Various Proteins Responsible for Survival, Inflammation, Cell Cycle, Angiogenesis, Migration, and Apoptosis of OSCC Cells and the Involvement of Multiple Signaling Pathways in the Mode of Action. Studies have evidenced that the upregulation of various proteins like MMP-2, COX-2, VEGF, Akt, NF-κB, CXCR-4, Bcl-2, Survivin, mTOR, and STAT-3 are responsible for enhanced proliferation, survival, angiogenesis, invasion and migration in cancer cells. However, the effect of DI on these gene products in human OSCC cells has not yet been elucidated. COX-2 catalyzes the first step in the synthesis of prostanoids and is often linked with carcinogenesis and inflammatory diseases. It promotes angiogenesis, migration, invasion of tumors, and deregulates apoptosis. As compared to healthy subjects, a significant upsurge in the expression of COX-2 was seen in cancer patients and patients with premalignant lesions.[45−49] Furthermore, survivin is known to play a critical role in cell survival by regulating cell division and apoptosis. It has been noted that the upregulation of survivin is frequently observed in OSCC samples. This protein is essential for in the development of OSCC and, and it is mostly associated with the more aggressive form.[50−52] VEGF-A is a 46 kDa heparin-binding homodimeric glycoprotein. It respectively binds to its receptor to promote endothelial cell differentiation and proliferation. Many studies have demonstrated the increase in the expression of VEGFs in different types of

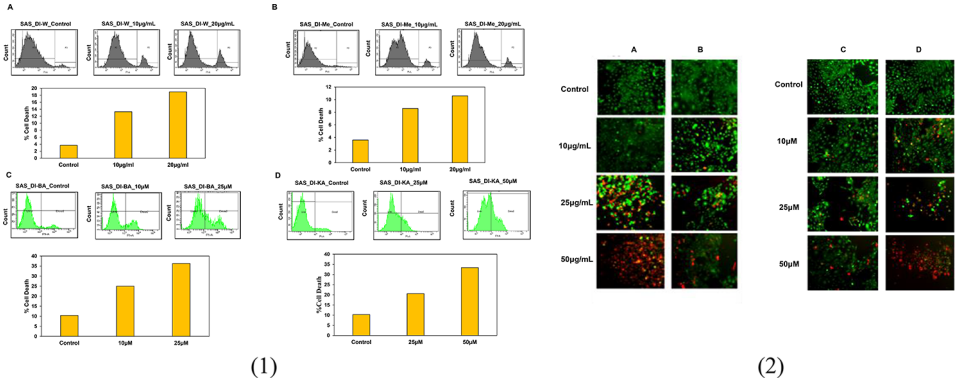

Figure 6. (1) Induction of cell death in SAS cells by (A) DI-H_2O Ext, (B) DI-ME Ext, (C) BA, and (D) KA. Cells were treated with the indicated concentrations for 72 h, followed by PI staining and FACS analysis for the cell death profile. (2) Live and dead assay was performed to evaluate the cytotoxic effect of the indicated concentrations of (A) DI-H_2O Ext, (B) DI-ME Ext, (C) BA, and (D) KA on SAS cells.

https://dx.doi.org/10.1021/acsptsci.1c00011
ACS Pharmacol. Transl. Sci. 2021, 4, 834−847

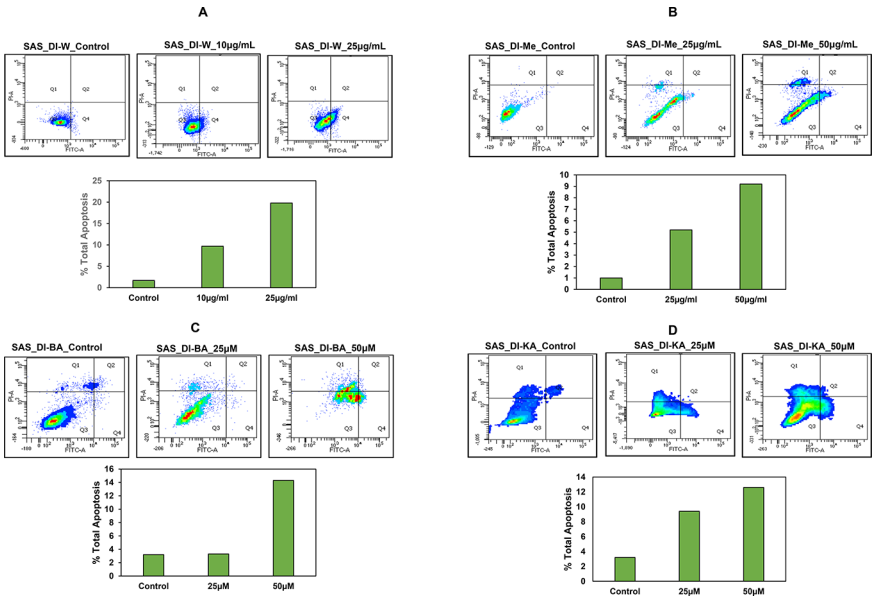

Figure 7. Induction of apoptosis in SAS cells upon treatment with (A) DI-H_2O Ext, (B) DI-ME Ext, (C) BA, and (D) KA. Cells were treated with the indicated concentrations for 72 h, followed by Annexin V staining and FACS analysis.

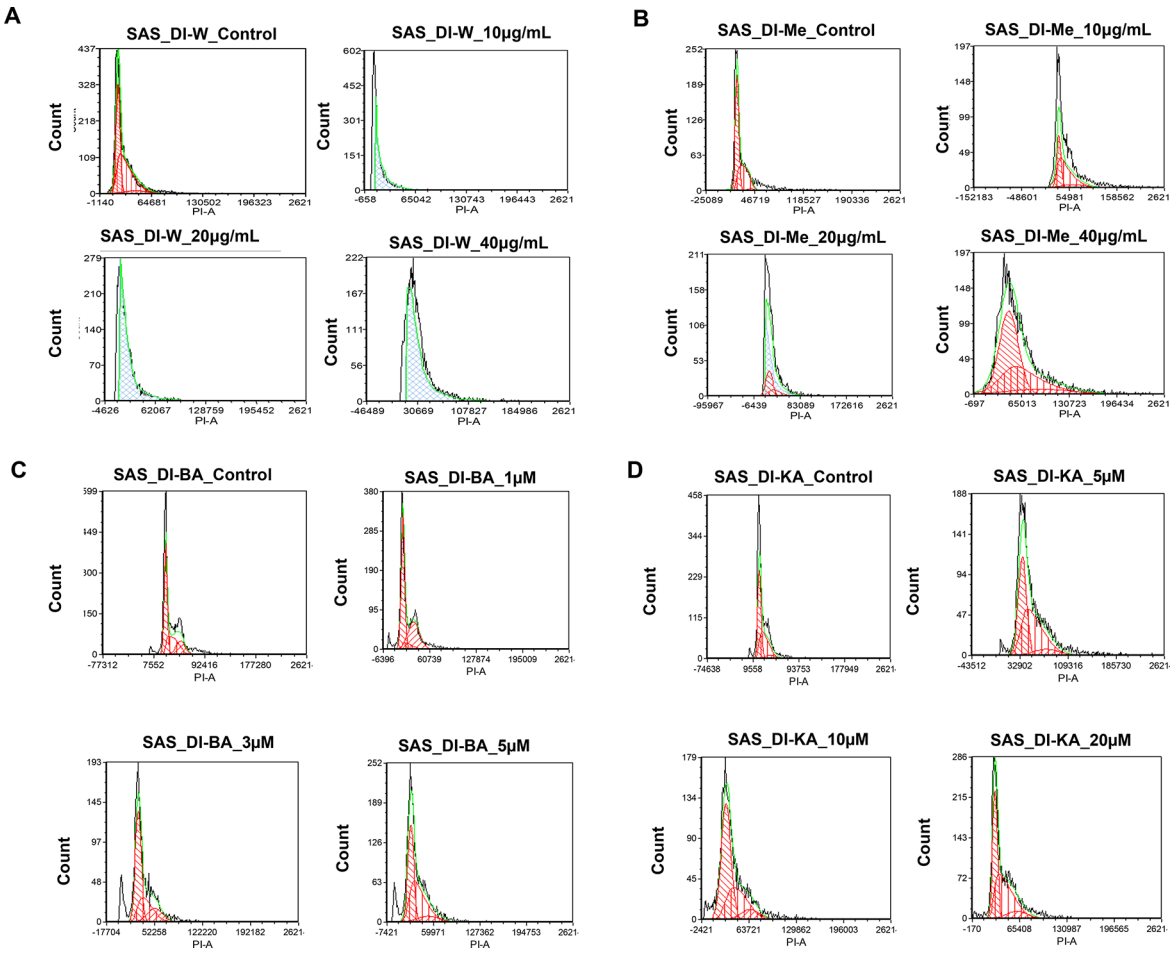

Figure 8. Induction of cell cycle arrest in SAS cells by (A) DI-H_2O Ext, (B) DI-ME Ext, (C) BA, and (D) KA. Percentages of each cell cycle phase were obtained using FCS Express software.

carcinoma. Macrophages, neutrophils, and fibroblasts, upon stimulation by the TGF-β and IL-8, secrete MMPs, and maintain the bioavailability of growth factors, thus promoting cancer cell proliferation. Furthermore, MMPs cleave the FAS receptors, and modulate the function of natural killer cells and the apoptosis mechanism. They are also known to promote

https://dx.doi.org/10.1021/acsptsci.1c00011
ACS Pharmacol. Transl. Sci. 2021, 4, 834−847

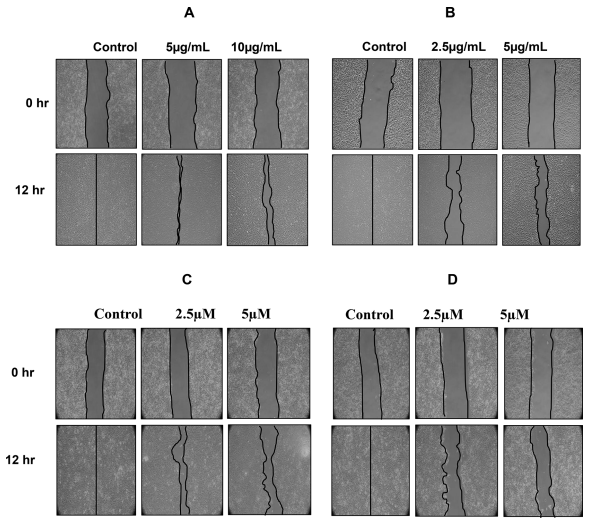

Figure 9. Inhibition of the migration of SAS cells upon treatment with (A) DI-H_2O Ext, (B) DI-ME Ext, (C) BA, and (D) KA. Cells were scratch-wounded and then treated with the indicated concentrations, followed by the recording of wound areas at different timepoints.

angiogenesis and metastasis. Various studies have shown that MMP-2 and MMP-9 are potential diagnostic markers for oral cancer detection.[53−56] In addition, CXCR4 overexpression in cancer cells contributes to tumor growth, proliferation, invasion, angiogenesis, metastasis, relapse, and chemoresistance. CXCR4 antagonism disrupts tumor-stromal interactions, reduces tumor growth and metastatic burden, and sensitizes cancer cells to cytotoxic drugs. CXCR4 is the target for not only therapeutic interference but it is also an important candidate for noninvasive checking of disease progression.[57] Also, Bcl-2 family proteins that regulate the intrinsic mitochondrial apoptosis pathway are activated in response to several stress stimuli, including growth-factor deprivation, cytokine-withdrawal, Ca^{2+}-flux, or DNA-damage, caused by UV or gamma-irradiation, but they can also contribute to cell death triggered by members of the tumor necrosis factor family member such as FAS, TNF, or TRAIL. Deregulation of Bcl-2 protein is a frequent feature of human malignant diseases and causal for therapy resistance.[58,59] NF-κB plays an essential role in inflammatory and immune responses and controls the expression of multiple genes associated with different hallmarks of cancer. The effect of DI on NF-κB as well as the diverse gene products regulated by NF-κB in human OSCC cells has not been elucidated yet. Therefore, in our study, we tried to explicate the effect of DI extracts, BA and KA on the expression of these proteins (Figure 10). Our findings revealed that the SAS cells treated with DI-H_2O Ext exhibited downregulation of VEGF-A, survivin and Bcl-2 via inhibition of the STAT3 pathway. However, similar trend was not observed in case of CXCR4. In addition, SAS cells treated with DI-ME Ext demonstrated downregulation of p-mTOR (S2448), and p-STAT-3 (S727), the crucial constituents of the Akt/mTOR and JAK/STAT signaling cascade. Besides, this extract was also found to inhibit the expression of CXCR4. Further, Western blot analysis showed that the DI constituents,

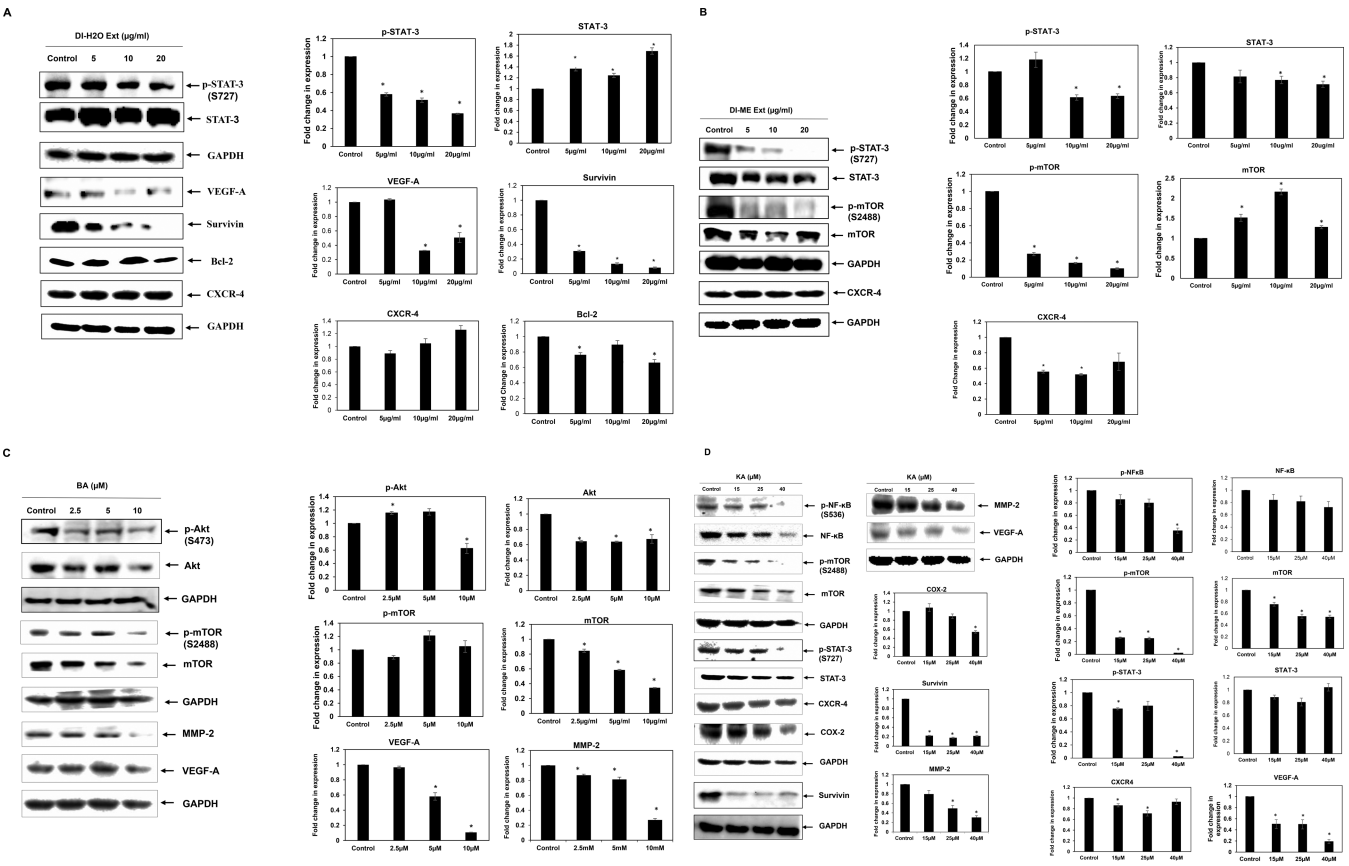

Figure 10. Expression of various proteins in SAS cells upon treatment with (A) DI-H_2O Ext, (B) DI-ME Ext, (C) BA, and (D) KA as examined by Western blot analysis. GADPH was used as housekeeping control.

https://dx.doi.org/10.1021/acsptsci.1c00011
ACS Pharmacol. Transl. Sci. 2021, 4, 834−847

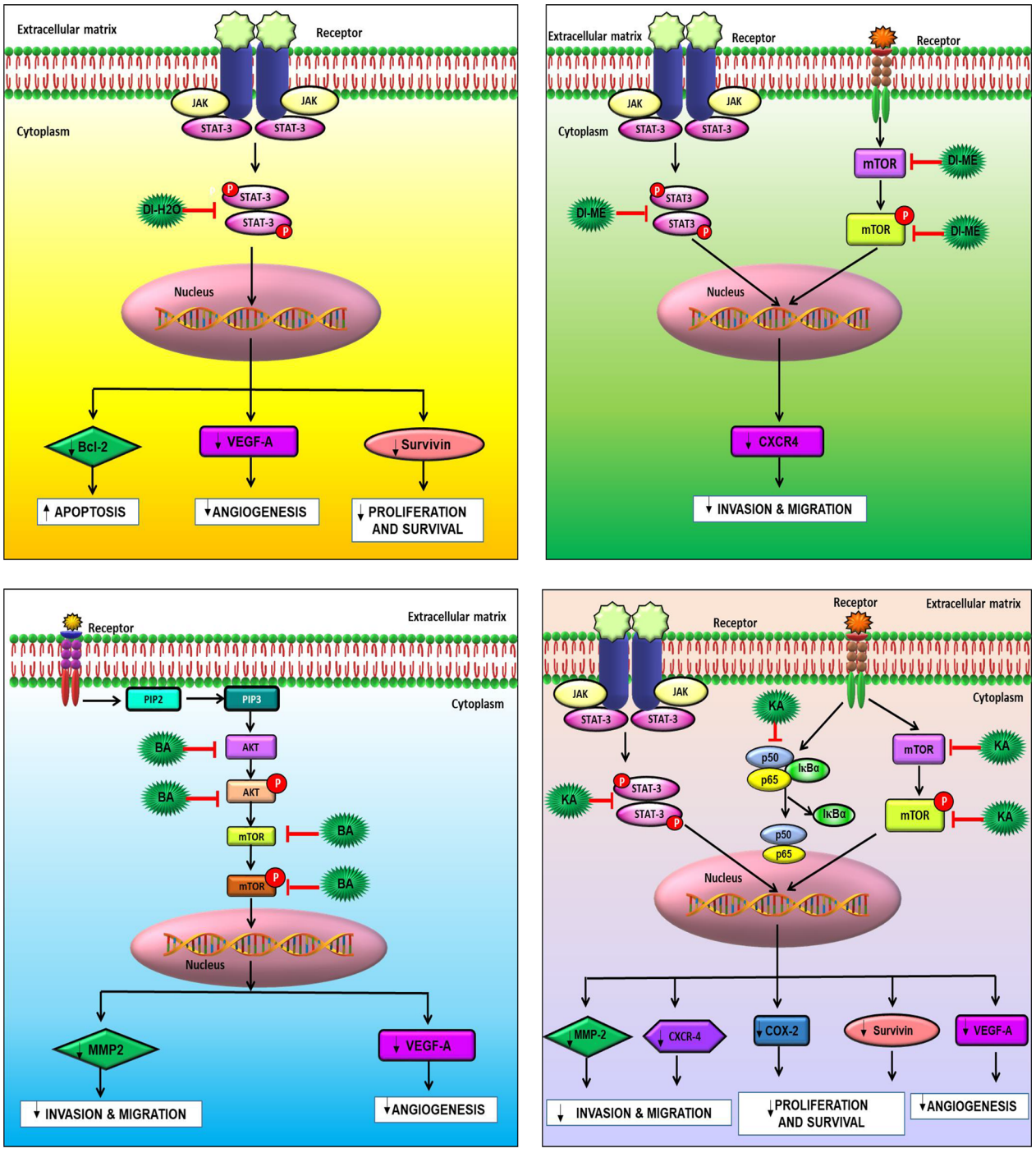

Figure 11. Pathway deciphering the proposed mechanistic mode of action with (A) DI-H_2O Ext, (B) DI-ME Ext, (C) BA, and (D) KA treatment in SAS cells.

BA caused dose-dependent downregulation of the expression of VEGF-A and MMP-2 via inhibition of the Akt/mTOR pathway. Similarly, KA was found to reduce the levels of COX-2, survivin, MMP-2 and VEGF-A through modulation of the NF-κB, mTOR and STAT3 pathways. A decrease of Bcl-2 expression was observed in DI-H_2O Ext treated SAS cells, indicating that the activation of the mitochondria-dependent apoptotic pathway, at least in part, plays a role in DI-induced apoptosis. Akt1 is a crucial signaling protein involved in cellular survival pathways. It regulates survival by inhibiting apoptosis. The transcription factor NF-κB is constitutively expressed in head and neck squamous cell carcinoma (HNSCC), and the persistent expression of this protein is one of the root causes of the cancer cell proliferation, survival, invasion, metastasis, and poor survival of patients. Our results showed that the phosphorylated forms of Akt1 and NF-κB were significantly downregulated upon treatment with BA and KA respectively. It is possible that both the p-Akt1(S473) and p-NF-κB (S536) proteins are intracellular targets of DI that mediates its cytotoxic effects on SAS cells. Taken together, our results showed that the DI extracts and their active constituents, BA and KA modulated the expression of several critical proteins involved in the development and progression of OSCC (Figure

https://dx.doi.org/10.1021/acsptsci.1c00011
ACS Pharmacol. Transl. Sci. 2021, 4, 834−847

11). These results provide an insight into the precise mechanism of action of DI and its constituents (Figure 11).

In summary, we have interpreted indigenous knowledge with scientific criteria and identified new cytotoxic agents against OSCC. The fruit extracts of the ethnomedicinal plant DI might vanquish the adverse side effects of conventional modalities of treatment. In order to recognize the bioactive scaffolds in the plant extract, we performed detailed phytochemical profiling. Ten compounds were isolated and characterized, out of which, five compounds, namely, koetjapic acid, palmarumycin JC1, ferulic acid, 3-oxykojic acid, and 2-(1′,2′dihydroxy)-kojic acid, were reported for the first time from this species. All the isolated molecules were screened through preliminary antiproliferative assay and the leads, BA and KA were identified. They were again subjected to virtual screening based on ligand binding affinity and molecular dynamic simulations for providing theoretical support to the scientific validation. Both of the selected candidates displayed significant anticancer potential *in vitro* by imparting antiproliferative, cytotoxic, anti-clonogenic, anti-metastatic, and apoptotic effects. Our findings were further supported by the reduced expression of various proteins involved in the development and progression of OSCC. However, further *in vivo* studies are required to validate our findings and also elucidate the precise mechanism of action, which may provide a basis for developing chemopreventive and chemotherapeutic strategies for the better management of OSCC.

EXPERIMENTAL SECTION

Plant Material. Fruits of DI were collected from Guwahati, Assam, and were identified by the taxonomists of Jawaharlal Nehru Botanical Garden of India, Palode, Thiruvananthapuram, Kerala. A voucher specimen number JNTBGRI 93635 was deposited at the herbarium of JNTBGRI, Kerala.

Cell Line. The OSCC cell line, SAS, was obtained from National Center for Cell Sciences (NCCS, Pune, India). The cells were maintained in DMEM supplemented with 10% heat-inactivated FBS and 1% Penstrep. The cells were grown in an incubator under optimum conditions of 5% CO_2 and temperature at 37 °C.

Reagents. Penstrep, Trypsin EDTA, DMEM medium, and FBS were obtained from Gibco, USA. MTT and PI were obtained from Invitrogen and Sigma-Aldrich respectively, while DMSO used was procured from Merck Life Science Pvt. Ltd. The live and dead assay kit was obtained from Invitrogen, USA. Crystal violet was procured from SRL Pvt. Ltd., India. The Optiblot ECL Detection Kit was procured from Abcam, Cambridge, USA.

Extraction of DI Fruits. Fruits and leaves of DI were collected in March 2018. These were thoroughly cleaned, dried (in an oven maintained at a temperature of 50 °C for 3 days) and powdered. A 1 kg sample of the powdered fruits was extracted with methanol (2.5 L × 48 h) at room temperature thrice and was filtered. The completion of extraction was checked with TLC. The filtrate was concentrated under reduced pressure using a Heidolph rotary evaporator at a temperature of 50 °C yielded 45 g of crude extract. The residue thus obtained was further extracted with water, lyophilized, and yielded 11 g of aqueous extract.

Isolation of Phytochemicals from Methanol Extract. TLC of the methanol extract in various combinations of *n*-hexane−ethyl acetate was studied. The residue was subjected to silica gel (100−200 mesh, Merck) column chromatography (CC) at different compositions of hexane, ethyl acetate, and methanol to afford 50 fractions (fractions 1−50). Each of these pooled fractions was concentrated by removing the solvent under reduced pressure using a Heidolph rotary evaporator.

Compound **1** (*β*-sitosterol, 10 mg) was obtained from fractions 1−3 via CC using 5% ethyl acetate−hexane, which recrystallized as white needle-shaped crystals with the same polarity.

Compound **2** (*n*-hentriacontanol, 7 mg) showed an intense spot in a cerium sulfate/phosphoric acid charring solution and was obtained as a white solid in 10% ethyl acetate−hexane.

Compound **3** (lupeol, 20 mg) was isolated from fraction 9 in 20% ethyl acetate−hexane and was further subjected to crystallization.

Compound **4** (betulinic acid, 4g) was obtained from 30% ethyl acetate in hexane as white solid, which was identified as the marker compound of the species.

Compound **5** (koetjapic acid, 17 mg) was isolated from a pool of fractions 30−34 by Sephadex LH 20 column with methanol as the eluent.

TLC of fractions 35−38 eluted from the column in 50−60% ethyl acetate in hexane showed an intense UV active spot, which was further purified by repeated CC by using sephadex LH 20 in methanol, yielding compound **6** (ferulic acid, 15 mg).

Compound **7** (palmarumycins JC1, 40 mg) eluted in 70% ethyl acetate in hexane, which was further purified by using sephadex LH 20 and recrystallized in methanol.

Compound **8** (3-oxykojic acid, 45 mg) and compound **9** ((2-(1′,2′-dihydroxy)-kojic acid, 30 mg) were obtained as a mixture of both from fractions 42−44, which were further purified by using Sephadex LH 20.

Compound **10** (*β*-sitosterol-*β*-D-glucopyranoside, 30 mg) was obtained from fractions 45−50 as an amorphous solid and was further purified by precipitation using acetone. All molecules were identified by ^{1}H and ^{13}C NMR spectra and HR-ESIMS (Tables S1−S10).

Characterization of Phytochemicals. NMR spectra were recorded on Bruker Avance AMX 500 MHz NMR spectrometer. Chemical shift was reported in parts per million using TMS as an internal standard with solvent residual peaks ($CDCl_3$: δ_H −7.26 ppm, δ_C −77.3 ppm), (DMSO-d_6: δ_H −2.50 ppm, δ_C −39.5 ppm), and (acetone-d_6: δ_H −2.05 ppm, δ_C −29.8 ppm). Multiplicities were given as s (singlet); d (doublet); t (triplet); q (quartet); dd (double doublet); and m (multiplet). Coupling constant, *J*, was expressed in Hz. Optical rotation was recorded on Jasco P-1020 polarimeter, and absorbance was recorded on a UV 1800 Shimadzu UV Spectrophotometer. Mass spectra were recorded under ESI-HRMS at 60 000 resolution on a Thermo Scientific Exactive Column, and IR spectra were recorded on Bruker Alpha FT-IR spectrometer. All solvents used for UV, IR, MS, and chromatography were purchased from Sigma-Aldrich and Merck (HPLC-grade). For CC, silica gel with different mesh sizes (100−200 and 230−400) and Sephadex-LH 20 were used.

Computational Screening and Molecular Dynamics Simulation. The optimization and minimization of the proteins, binding site analysis, receptor grid generation, ligand conformation generation, ADME/T screening, molecular docking, and dynamics were done with Schrödinger suite 2020−1.[60] For this, protein preparation wizard, Sitemap, LigPrep, QikProp, Glide XP docking, and Desmond tools were used in Maestro 11.2 interface in OPLS-2005 force field.[61] The

https://dx.doi.org/10.1021/acsptsci.1c00011
ACS Pharmacol. Transl. Sci. 2021, 4, 834−847

crystal structures of the proteins were retrieved from the RCSB Protein Data Bank: protein kinase B, Akt (PDB ID: 1O6L); mammalian target of rapamycin, mTOR (PDB ID: 4JSP); matrix metalloproteinase-2, MMP-2 (PDB ID: 3AYU); vascular endothelial growth factor-A, VEGF-A (PDB ID: 1FLT); nuclear factor kappa-light-chain-enhancer of activated B cells, NF-κB (PDB ID: 1SVC); signal transducer and activator of transcription 3, STAT-3 (PDB ID: 6NJS); C-X-C chemokine receptor type 4, CXCR-4 (PDB ID: 3ODU), cyclooxygenase-2, COX-2 (PDB ID: 5IKQ); and survivin (PDB ID: 1E31).[62] All these proteins were refined by adding hydrogens/missing side chains, optimized, and minimized. The phosphorylated forms of the Akt, mTOR, NF-κB, and STAT-3 were generated successively by adding a phosphate group to the corresponding serine residues using build structure protocol. Site map analysis was carried out to identify the suitable binding pockets in the case of these receptors, and the grids were generated around site 1 which were used for further docking. The different conformers of the BA and KA were generated using LigPrep module and screened their ADME/T (Absorption, Distribution, Metabolism, and Excretion/Toxicity) properties by QikProp analysis. The docking simulations were done by Glide docking, and the binding affinities were ranked using docking score (D-score) and glide score (G-score). Molecular dynamics simulations further analyzed the best ones for 10 000 ps using the Desmond module of Schrödinger suite under OPLS-2005 force field.

Cell Proliferation Assay. A total of 2×10^3 SAS cells per 100 μL media were seeded into each well of two 96-well plates and incubated for 24 h. The cells were then treated with different concentrations of the DI-H_2O Ext, DI-ME Ext, BA, and KA individually, and the MTT assay was performed at 0 and 72 h. A 10 μL aliquot of MTT at a concentration of 5 mg/mL in PBS was added to each well and incubated for 2 h. Next, the cell culture medium was discarded, and 100 μL of DMSO was added to each well and incubated for 1 h in the dark. Color conversion of the MTT reaction was measured with a microplate reader at a wavelength of 570 nm. Control cells were defined as 100% proliferation, and the percentage proliferation was calculated to the following formula: (Absorption of treated cells × 100)/(Absorption of control cells (untreated)).

Colony-Forming Assay. A total of 1×10^3 cells per 2 mL were seeded in a 6-well plate and incubated for 24 h. The cells were then treated with DI-H_2O Ext, DI-ME Ext, BA, and KA separately and incubated for another 24 h. The next day, the media of the wells were replaced with fresh media, and the cells were allowed to form colonies for 9 days. On 9th day, colonies were fixed with ethanol, stained with 0.3% crystal violet (SRL Pvt. Ltd., India) solution for 20 min and washed. Images were captured for each well and the number of colonies was quantified using ImageJ software.

Cell Death Analysis. A total of 2×10^4 SAS cells per 2 mL of media were seeded in a 6-well plate and incubated for 24 h, followed by treatment with different concentrations of DI-H_2O Ext, DI-ME Ext, BA, and KA individually. After 72 h of drug treatment, the media from the wells were collected in labeled 5 × 77 mm^2 polystyrene test tubes. Adhered cells were washed with PBS, trypsinized, and collected in their respective tubes. The cell suspension was then centrifuged at 4000 rpm for 10 min at 4 °C. After centrifugation, the supernatant was discarded, and the pellet was washed with 1 mL of PBS and centrifuged at 4000 rpm for 10 min, and the step was repeated twice. Finally, the pellet was suspended in 495 μL of PBS, and 5 μL of PI (Sigma-Aldrich) dye was added. The cells were then analyzed in BD FACS Diva software. PI dye is impermeable to the live cells as they have an intact cell membrane and thus emit less fluorescence; however, PI can easily penetrate the dead cells because of the damaged plasma membrane, thereby emitting a high red fluorescence.

Live and Dead Assay. DI-mediated cell death in SAS cells was studied using the Live−Dead assay kit (Invitrogen, USA). The kit contains two fluorescent dyes, calcein-AM and PI. In principle, calcein-AM can enter any cells but labels only live cells. It is converted by cellular cytoplasmic esterases to a highly green-fluorescent calcein. PI is excluded by live cells with an intact membrane but enters dead cells with a broken membrane to stain their nuclei red. Therefore, live cells fluoresce green, whereas dead cells fluoresce red. SAS cells were seeded at 2000 cells per 100 μL of media in 96-well tissue culture plates. After 24 h, the cells were treated with DI-H_2O Ext, DI-ME Ext, BA, and KA individually. Cells were then stained with the live/dead reagent and incubated at 37 °C in the dark for 20 min. Cells were then analyzed under an inverted fluorescence microscope (Olympus, Japan).

Apoptosis Assay. Apoptosis is marked by the translocation and accumulation of the membrane phospholipid phosphatidylserine from the cytoplasmic edge of the membrane to the extracellular surface. The membrane perturbation can be detected by using Annexin V which binds to the phosphatidylserine of the apoptotic cells. A total of 5×10^4 SAS cells per 2 mL of media were seeded in a 6-well plate and incubated for 24 h, followed by treatment with different concentrations of DI-H_2O Ext, DI-ME Ext, BA, and KA individually. After 72 h of drug treatment, the media from the wells were collected in labeled 5 × 77 mm^2 polystyrene test tubes. Adhered cells were washed with PBS, trypsinized, and collected in their respective tubes. The cell suspension was then centrifuged at 4000 rpm for 10 min at 4 °C. After centrifugation, the supernatant was discarded, and the pellet was washed with 1 mL of PBS and centrifuged at 4000 rpm for 10 min. The PBS was discarded, and 20 μL of binding buffer was added to the tubes and the tubes were centrifuged again. Then the untreated control was divided into unstained (does not contain either PI or Annexin V) and double-stained (contain both the dyes) tubes, and the positive control was divided into PI-positive and Annexin V-positive tubes. A 2.5 μL aliquot of Annexin V added to all the tubes except the unstained and PI-positive ones and incubated in the dark for 20 min containing different concentrations of DI. The tubes were incubated in dark for 20 min. Centrifugation was done again, and the supernatant is discarded. A 20 μL aliquot of binding buffer is added, and 2.5 μL of PI (Sigma-Aldrich) dye was added. The cells were then analyzed in BD FACS Cell Quest software.

Cell Cycle Analysis. A total of 2×10^5 SAS cells per 2 mL of media were seeded in a 6-well plate and incubated overnight for cell adhesion. The cells were then treated with different concentrations of DI, and the untreated sample was used as a control. Following 24 h of individual treatment of DI-H_2O Ext, DI-ME Ext, BA, and KA , the media was collected in polystyrene tubes, and the adhered cells were washed with PBS twice. Then, 300 μL of trypsin was added to detach the cells. The detached cells were harvested in their respective tubes and centrifuged at 4000 rpm for 10 min at 4 °C. The supernatant was discarded, and the pellet was washed with 1 mL of PBS

https://dx.doi.org/10.1021/acsptsci.1c00011
ACS Pharmacol. Transl. Sci. 2021, 4, 834−847

and centrifuged at 4000 rpm for 10 min at 4 °C. Then the supernatant was discarded, and 5 mL of 70% ethanol was dropwise added to the pellet under constant vortexing and kept for overnight incubation at 4 °C for fixation. The next day, the suspension was centrifuged at 4000 rpm for 10 min at 4 °C, and the supernatant was discarded. Following the removal of ethanol by centrifugation, the cells were washed twice with PBS and stained with PI/RNase solution for 30 min in the dark. Cell cycle distribution was detected using FACS Celesta (Becton-Dickinson, Franklin Lakes, NJ), and the data were analyzed using FCS Express (BD Biosciences). The fluorescence intensity of the stained cells correlates with the amount of DNA they contain.

Cell Migration Assay. A total of 5×10^5 SAS cells per 2 mL of media were seeded in a 6-well plate and incubated for 12 h to form the monolayer. After the monolayer was formed, the media was replaced with serum-free media and incubated for 8 h. Thereafter, the media was removed, and a vertical scratch or wound was made with the help of a 200 μL tip at the center of the well. The wells were then washed with PBS twice to remove the debris. Cells were then treated with different concentrations of DI-H_2O Ext, DI-ME Ext, BA, and KA individually. The untreated cells were used as control. The directional migration of SAS cells was observed under an inverted microscope (Nikon T1-SM, Tokyo, Japan), and images were taken at 0 and 12 or 24 h depending upon the healing timepoint of the wound. Images were compared to quantify the migration of SAS cells after treatment.

Western Blot Analysis. A total of 6×10^5 cells per 3 mL of media were seeded in 60 mm culture plates and were allowed to grow for 24 h. The cells were then treated with different concentrations of DI-H_2O Ext, DI-ME Ext, BA, and KA individually and incubated for the next 24 h. Protein was isolated from respective treatment plates using lysis buffer (20 mM HEPES, 2 mM EDTA, 250 mM NaCl, and 0.1% NP40) in the presence of protease inhibitors (2 μg/mL leupeptin hemisulfate, 2 μg/mL aprotinin, 1 mM PMSF, and 1 mM DTT) and quantified using Bradford's reagent. Equal amount of protein (30 μg) was mixed with 5× Laemmli Buffer (250 mM Tris-HCl, 10% SDS, 30% glycerol, 5% β-mercaptoethanol, and 0.02% bromophenol blue) and separated by 12% SDS-PAGE and transferred to nitrocellulose membrane (Biorad) by using a Trans-blot Turbo (Biorad), the membrane was blocked with 5% nonfat skim milk in tris-buffered saline containing 1% tween 20 (TBST). For the phospho-antibodies, the membranes were treated with 5% BSA in tris-buffered saline containing 1% tween 20 to block the nonspecific binding sites. The membranes were then incubated with primary antibodies for MMP-2, COX-2, VEGF-A, Akt1, p-Akt, NF-κB, p-NF-κB, CXCR-4, cyclin D1, Bcl-2, survivin, mTOR, p-mTOR, STAT-3, p-STAT-3, and GAPDH overnight at 4 °C. Afterwards, the blots were washed with 1X TBST buffer and then incubated with horseradish peroxidase conjugated secondary antibody for 2 h at room temperature. The bands representing different proteins were visualized with the help of Clarity Western ECL Substrate (Biorad) in a ChemiDoc XRS System (Biorad). GAPDH was used as the housekeeping control.

Statistical Analysis. Statistical analysis was performed using Student's t test. All the data are represented as mean ± standard error (SE). $p < 0.05$ was defined as statistically significant.

■ ASSOCIATED CONTENT

Supporting Information

The Supporting Information is available free of charge at https://pubs.acs.org/doi/10.1021/acsptsci.1c00011.

Isolation procedure, characterization techniques, preliminary MTT screening of both extracts and isolated compounds, computational screening of compounds discussed (PDF)

■ AUTHOR INFORMATION

Corresponding Authors

Ajaikumar B. Kunnumakkara − *Cancer Biology Laboratory and DBT-AIST International Center for Translational & Environmental Research (DAICENTER), Department of Biosciences and Bioengineering, Indian Institute of Technology, Guwahati 781 039, Assam, India;* orcid.org/0000-0001-9121-6816; Email: kunnumakkara@iitg.ac.in

Radhakrishnan Kokkuvayil Vasu − *Chemical Sciences and Technology Division, CSIR-National Institute for Interdisciplinary Science and Technology (CSIR-NIIST), Thiruvananthapuram 695019, India; Academy of Scientific and Innovative Research (AcSIR), Ghaziabad 201002, India;* orcid.org/0000-0001-8909-3175; Email: radhu@niist.res.in

Authors

Maniyamma Aswathy − *Chemical Sciences and Technology Division, CSIR-National Institute for Interdisciplinary Science and Technology (CSIR-NIIST), Thiruvananthapuram 695019, India; Academy of Scientific and Innovative Research (AcSIR), Ghaziabad 201002, India*

Kishore Banik − *Cancer Biology Laboratory and DBT-AIST International Center for Translational & Environmental Research (DAICENTER), Department of Biosciences and Bioengineering, Indian Institute of Technology, Guwahati 781 039, Assam, India;* orcid.org/0000-0003-2497-8313

Dey Parama − *Cancer Biology Laboratory and DBT-AIST International Center for Translational & Environmental Research (DAICENTER), Department of Biosciences and Bioengineering, Indian Institute of Technology, Guwahati 781 039, Assam, India*

Parameswaran Sasikumar − *Chemical Sciences and Technology Division, CSIR-National Institute for Interdisciplinary Science and Technology (CSIR-NIIST), Thiruvananthapuram 695019, India*

Choudhary Harsha − *Cancer Biology Laboratory and DBT-AIST International Center for Translational & Environmental Research (DAICENTER), Department of Biosciences and Bioengineering, Indian Institute of Technology, Guwahati 781 039, Assam, India*

Anuja Gracy Joseph − *Chemical Sciences and Technology Division, CSIR-National Institute for Interdisciplinary Science and Technology (CSIR-NIIST), Thiruvananthapuram 695019, India; Academy of Scientific and Innovative Research (AcSIR), Ghaziabad 201002, India*

Daisy R. Sherin − *Centre for Computational Modeling and Data Engineering, Indian Institute of Information Technology and Management-Kerala (IIITM-K), Thiruvananthapuram 695581, India*

Manojkumar K. Thanathu − *Centre for Computational Modeling and Data Engineering, Indian Institute of*

https://dx.doi.org/10.1021/acsptsci.1c00011
ACS Pharmacol. Transl. Sci. 2021, 4, 834−847

Information Technology and Management-Kerala (IIITM-K), Thiruvananthapuram 695581, India

Complete contact information is available at: https://pubs.acs.org/10.1021/acsptsci.1c00011

Author Contributions

#A.M., K.B., and D.P. contributed equally to this work.

Notes

The authors declare no competing financial interest.

■ ACKNOWLEDGMENTS

CSIR Ph.D. student M.A. thanks CSIR for research fellowship. K.B. acknowledges UGC for providing fellowship. M.A. thanks Mathew Dan, Senior Scientist, Plant Genetics Resources Division, JNTBGRI, for providing plant material. A.B.K. acknowledges BT/556/NE/U-Excel/2016 project awarded by Department of Biotechnology, Govt. of India.

■ ABBREVIATIONS

Bcl-2, B-cell lymphoma 2; BSA, Bovine serum albumin; Ca^{++}, Calcium ion; CC, Column chromatography; COX-2, cyclo-oxygenase 2; CXCR4, C-X-C chemokine receptor type 4; DI, *Dillenia indica*; DMEM, Dulbecco's modified eagle's medium; DMSO, Dimethyl sulfoxide; DTT, Dithiothreitol; EDTA, Ethylenediaminetetraacetic acid; EGFR, Epidermal growth factor receptor; ESI, Electrospray ionization; FACS, Fluorescence-activated cell sorting; FBS, Fetal bovine serum; Fr., Fraction; GAPDH, Glyceraldehyde 3-phosphate dehydrogenase; HEPES, 4-(2-hydroxyethyl)-1-piperazineethanesulfonic acid; HPLC, High-performance liquid chromatography; HRMS, High-resolution electrospray ionization mass spectrometry; IL-8, Interleukin-8; IR, Infrared; JAK2, Janus kinase 2; MMPs, Matrix metalloproteinases; MS, Mass spectrometry; mTOR, Mammalian target of rapamycin; MTT, 3-(4,5-dimethylthiazol-2-yl)-2,5-diphenyltetrazolium bromide; NF-κB, Nuclear factor kappa B; NMR, Nuclear magnetic resonance; OSCC, Oral squamous cell carcinoma; p38 MAPK, p38 mitogen-activated protein kinase; PBS, Phosphate-buffered saline; PI, Propidium iodide; PMSF, Phenylmethylsulfonyl fluoride; SDS-PAGE, Sodium dodecyl sulfate polyacrylamide gel electrophoresis; STAT, Signal transducer and activator of transcription; TBST, Tris-buffered saline (TBS) and Polysorbate 20 (Tween 20); TLC, Thin-layer chromatography; TNF, Tumor necrosis factor; TRAIL, TNF-related apoptosis-inducing ligand; UV, Ultraviolet; VEGF, Vascular endothelial growth factor

■ REFERENCES

(1) Bray, F., Ferlay, J., Soerjomataram, I., Siegel, R. L., Torre, L. A., and Jemal, A. (2018) Global Cancer Statistics 2018: GLOBOCAN Estimates of Incidence and Mortality Worldwide for 36 Cancers in 185 Countries. *Ca-Cancer J. Clin. 68* (6), 394−424.

(2) Harsha, C., Banik, K., Ang, H. L., Girisa, S., Vikkurthi, R., Parama, D., Rana, V., Shabnam, B., Khatoon, E., Kumar, A. P., and Kunnumakkara, A. B. (2020) Targeting AKT/mTOR in Oral Cancer: Mechanisms and Advances in Clinical Trials. *Int. J. Mol. Sci. 21* (9), 3285.

(3) Singh, A. K., Roy, N. K., Bordoloi, D., Padmavathi, G., Banik, K., Khwairakpam, A. D., Kunnumakkara, A. B., and Sukumar, P. (2020) Orai-1 and Orai-2 regulate oral cancer cell migration and colonisation by suppressing Akt/mTOR/NF-κB signalling. *Life Sci. 261*, 118372.

(4) Kunnumakkara, A. B., Thakur, K. K., Rana, V., Bora, B., Banik, K., Khatoon, E., Sailo, B. L., Shabnam, B., Girisa, S., Gupta, S. C., and Aggarwal, B. B. (2019) Upside and Downside of Tumor Necrosis Factor Blockers for Treatment of Immune/Inflammatory Diseases. *Crit. Rev. Immunol. 39* (6), 439−479.

(5) Kunnumakkara, A. B., Harsha, C., Banik, K., Vikkurthi, R., Sailo, B. L., Bordoloi, D., Gupta, S. C., and Aggarwal, B. B. (2019) Is curcumin bioavailability a problem in humans: lessons from clinical trials. *Expert Opin. Drug Metab. Toxicol. 15* (9), 705−733.

(6) Bordoloi, D., Monisha, J., Roy, N. K., Padmavathi, G., Banik, K., Harsha, C., Wang, H., Kumar, A. P., Arfuso, F., and Kunnumakkara, A. B. (2019) An Investigation on the Therapeutic Potential of Butein, A Tretrahydroxychalcone Against Human Oral Squamous Cell Carcinoma. *Asian Pac.J. Cancer Prev. 20* (11), 3437−3446.

(7) Devi Khwairakpam, A., Monisha, J., Roy, N. K., Bordoloi, D., Padmavathi, G., Banik, K., Khatoon, E., and Kunnumakkara, A. B. (2019) Vietnamese coriander inhibits cell proliferation, survival and migration via suppression of Akt/mTOR pathway in oral squamous cell carcinoma. *J. Basic Clin. Physiol. Pharmacol 31* (3), 20190162.

(8) Roy, N. K., Parama, D., Banik, K., Bordoloi, D., Devi, A. K., Thakur, K. K., Padmavathi, G., Shakibaei, M., Fan, L., Sethi, G., and Kunnumakkara, A. B. (2019) An Update on Pharmacological Potential of Boswellic Acids against Chronic Diseases. *Int. J. Mol. Sci. 20* (17), 4101.

(9) Roy, N. K., Monisha, J., Padmavathi, G., Lalhruaitluanga, H., Kumar, N. S., Singh, A. K., Bordoloi, D., Baruah, M. N., Ahmed, G. N., Longkumar, I., Arfuso, F., Kumar, A. P., and Kunnumakkara, A. B. (2019) Isoform-Specific Role of Akt in Oral Squamous Cell Carcinoma. *Biomolecules 9* (7), 253.

(10) Kunnumakkara, A. B., Bordoloi, D., Sailo, B. L., Roy, N. K., Thakur, K. K., Banik, K., Shakibaei, M., Gupta, S. C., and Aggarwal, B. B. (2019) Cancer drug development: The missing links. *Exp. Biol. Med. 244* (8), 663−689.

(11) Shabnam, B., Padmavathi, G., Banik, K., Girisa, S., Monisha, J., Sethi, G., Fan, L., Wang, L., Mao, X., and Kunnumakkara, A. B. (2018) Sorcin a Potential Molecular Target for Cancer Therapy. *Transl. Oncol. 11* (6), 1379−1389.

(12) Monisha, J., Roy, N. K., Padmavathi, G., Banik, K., Bordoloi, D., Khwairakpam, A. D., Arfuso, F., Chinnathambi, A., Alahmadi, T. A., Alharbi, S. A., Sethi, G., Kumar, A. P., and Kunnumakkara, A. B. (2018) NGAL is Downregulated in Oral Squamous Cell Carcinoma and Leads to Increased Survival, Proliferation, Migration and Chemoresistance. *Cancers 10* (7), 228.

(13) Hanahan, D., and Weinberg, R. A. (2011) Hallmarks of cancer: the next generation. *Cell 144*, 646−674.

(14) Anand, P., Sundaram, C., Jhurani, S., Kunnumakkara, A. B., and Aggarwal, B. B. (2008) Curcumin and cancer: an "old-age" disease with an "age-old" solution. *Cancer Lett. 267*, 133−164.

(15) Dissanayaka, W. L., Pitiyage, G., Kumarasiri, P. V., Liyanage, R. L., Dias, K. D., and Tilakaratne, W. M. (2012) Clinical and histopathologic parameters in survival of oral squamous cell carcinoma. Oral Surg. *Oral Med. Oral Pathol. Oral Radiol. 113* (4), 518−525.

(16) Lee, J., Taneja, V., and Vassallo, R. (2012) Cigarette smoking and inflammation: cellular and molecular mechanisms. *J. Dent. Res. 91* (2), 142−149.

(17) Huang, M., Lu, J. J., Huang, M. Q., Bao, J. L., Chen, X. P., and Wang, Y. T. (2012) Terpenoids: natural products for cancer therapy. *Expert Opin. Invest. Drugs 21* (12), 1801−1818.

(18) Henamayee, S., Banik, K., Sailo, B. L., Shabnam, B., Harsha, C., Srilakshmi, S., Vgm, N., Baek, S. H., Ahn, K. S., and Kunnumakkara, A. B. (2020) Therapeutic Emergence of Rhein as a Potential Anti-cancer Drug: A Review of Its Molecular Targets and Anticancer Properties. *Molecules 25* (10), 2278.

(19) Parama, D., Boruah, M., Yachna, K., Rana, V., Banik, K., Harsha, C., Thakur, K. K., Dutta, U., Arya, A., Mao, X., Ahn, K. S., and Kunnumakkara, A. B. (2020) Diosgenin, a steroidal saponin, and its analogs: Effective therapies against different chronic diseases. *Life Sci. 260*, 118182.

(20) Khatoon, E., Banik, K., Harsha, C., Sailo, B. L., Thakur, K. K., Khwairakpam, A. D., Vikkurthi, R., Devi, T. B., Gupta, S. C., and

Kunnumakkara, A. B. (2020) Phytochemicals in cancer cell chemosensitization: Current knowledge and future perspectives. *Semin. Cancer Biol.* DOI: 10.1016/j.semcancer.2020.06.014.
(21) Banik, K., Ranaware, A. M., Harsha, C., Nitesh, T., Girisa, S., Deshpande, V., Fan, L., Nalawade, S. P., Sethi, G., and Kunnumakkara, A. B. (2020) Piceatannol: A natural stilbene for the prevention and treatment of cancer. *Pharmacol. Res. 153*, 104635.
(22) Kunnumakkara, A. B., Banik, K., Bordoloi, D., Harsha, C., Sailo, B. L., Padmavathi, G., Roy, N. K., Gupta, S. C., and Aggarwal, B. B. (2018) Googling the Guggul (Commiphora and Boswellia) for Prevention of Chronic Diseases. *Front. Pharmacol. 9*, 686.
(23) Ranaware, A. M., Banik, K., Deshpande, V., Padmavathi, G., Roy, N. K., Sethi, G., Fan, L., Kumar, A. P., and Kunnumakkara, A. B. (2018) Magnolol: A Neolignan from the Magnolia Family for the Prevention and Treatment of Cancer. *Int. J. Mol. Sci. 19* (8), 2362.
(24) Banik, K., Harsha, C., Bordoloi, D., Lalduhsaki Sailo, B., Sethi, G., Leong, H. C., Arfuso, F., Mishra, S., Wang, L., Kumar, A. P., and Kunnumakkara, A. B. (2018) Therapeutic potential of gambogic acid, a caged xanthone, to target cancer. *Cancer Lett. 416*, 75−86.
(25) Banik, K., Ranaware, A. M., Deshpande, V., Nalawade, S. P., Padmavathi, G., Bordoloi, D., Sailo, B. L., Shanmugam, M. K., Fan, L., Arfuso, F., Sethi, G., and Kunnumakkara, A. B. (2019) Honokiol for cancer therapeutics: A traditional medicine that can modulate multiple oncogenic targets. *Pharmacol. Res. 144*, 192−209.
(26) Sharma, H. K., Chhangte, L., and Dolui, A. K. (2001) Traditional medicinal plants in Mizoram, India. *Fitoterapia 72* (2), 146−161.
(27) Rai, P. K., and Lalramnghinglova, H. (2010) Lesser known ethnomedicinal plants of Mizoram, North East India: an Indo-Burma hotspot region. *J. Med. Plants Res. 4* (13), 1301−1307.
(28) Foo, J. B., Saiful Yazan, L., Tor, Y. S., Wibowo, A., Ismail, N., Armania, N., Cheah, Y. K., and Abdullah, R. (2016) Dillenia suffruticosa dichloromethane root extract induced apoptosis towards MDA-MB-231 triple-negative breast cancer cells. *J. Ethnopharmacol. 187*, 195−204.
(29) Foo, J. B., Saiful Yazan, L., Tor, Y. S., Wibowo, A., Ismail, N., How, C. W., Armania, N., Loh, S. P., Ismail, I. S., Cheah, Y. K., and Abdullah, R. (2015) Induction of cell cycle arrest and apoptosis by betulinic acid-rich fraction from Dillenia suffruticosa root in MCF-7 cells involved p53/p21 and mitochondrial signalling pathway. *J. Ethnopharmacol. 166*, 270−8.
(30) Tarak, D., Namsa, N. D., Tangjang, S., Arya, S. C., Rajbonshi, B., Samal, P. K., and Mandal, M. (2011) An inventory of the ethnobotanicals used as anti-diabetic by a rural community of Dhemaji district of Assam, Northeast India. *J. Ethnopharmacol. 138* (2), 345−350.
(31) Kritikar, K. R., and Basu, B. D. (2010) *Indian Medicinal Plants*, Vol. *II*, International Book Distributors, India.
(32) Abdille, M. H., Singh, R. P., Jayaprakasha, G. K., and Jena, B. S. (2005) Antioxidant activity of the extracts from Dillenia indica fruits. *Food Chem. 90* (4), 891−896.
(33) Prasad, P. R. C., Reddy, C. S., Raza, S. H., and Dutt, C. B. S. (2008) Folklore medicinal plants of north Andaman Islands, India. *Fitoterapia 79* (6), 458−464.
(34) Das, M., Sarma, B. P., Ahmed, G., Nirmala, C. B., and Choudhury, M. K. (2012) In vitro anti oxidant activity total phenolic content of *Dillenia indica* Garcinia penducalata, commonly used fruits in Assamese cuisine. *Free Radicals Antioxid. 2* (2), 30−36.
(35) Pavanasasivam, G., and Sultanbawa, M. U. S. (1975) Flavonoids of some Dilleniaceae species. *Phytochemistry 14*, 1127−1128.
(36) Banerji, N., Mjumder, P., and Dutta, N. I. (1975) A new pentacyclic triterpene lactone from *Dillenia indica*. *Phytochemistry 14*, 1447−1448.
(37) Suokas, E., Hase, T., Liaaen-Jensen, S.øv., Matsutaka, H., and Matsuno, T. (1978) Dry Ozonation of 3beta,28-Diacetoxylupane. A Comment on the Structure of a Pentacyclic Triterpenoid Lactone from Dillenia indica (Linn.). *Acta Chem. Scand. 32b*, 623−624.
(38) Fulda, S., Jeremias, I., Steiner, H. H., Pietsch, T., and Debatin, K.-M. (1999) Betulinic acid: A new cytotoxic agent against malignant brain-tumor cells. *Int. J. Cancer 82*, 435−441.
(39) Kumar, P., Bhadauria, A. S., Singh, A. K., and Saha, S. (2018) Betulinic acid as apoptosis activator: Molecular mechanisms, mathematical modeling and chemical modifications. *Life Sci. 209*, 24−33.
(40) Cai, Y., Zheng, Y., Gu, J., Wang, S., Wang, N., Yang, B., Zhang, F., Wang, D., Fu, W., and Wang, Z. (2018) Betulinic acid chemosensitizes breast cancer by triggering ER stress-mediated apoptosis by directly targeting GRP78. *Cell Death Dis. 9*, 636.
(41) Mertens-Talcott, S. U., Noratto, G. D., Li, X., Angel-Morales, G., Bertoldi, M. C., and Safe, S. (2013) Betulinic Acid Decreases ER-Negative Breast Cancer Cell Growth In Vitro and In Vivo: Role of Sp Transcription Factors and MicroRNA-27a:ZBTB10. *Mol. Carcinog. 52*, 591.
(42) Yang, C., Li, Y., Fu, L., Jiang, T., and Meng, F. (2018) Betulinic acid induces apoptosis and inhibits metastasis of human renal carcinoma cells in vitro and in vivo. *J. Cell. Biochem. 119*, 8611.
(43) Shen, H., Liu, L., Yang, Y., Xun, W., Wei, K., and Zeng, G. (2017) Betulinic Acid Inhibits Cell Proliferation in Human Oral Squamous Cell Carcinoma via Modulating ROS-Regulated p53 Signaling. *Oncol. Res. 25* (7), 1141−1152.
(44) Abubakar, S., Khor, B.-K., Khaw, K.-Y., Murugaiyah, V., and Chan, K.-L. (2021) Cholinesterase inhibitory potential of Dillenia suffruticosa chemical constituents and protective effect against Aβ-induced toxicity in transgenic Caenorhabditis elegans model. *Phytomedicine Plus. 1* (1), 100022.
(45) Zeng, A., Hua, H., Liu, L., and Zhao, J. (2019) Betulinic acid induces apoptosis and inhibits metastasis of human colorectal cancer cells in vitro and in vivo. *Bioorg. Med. Chem. 27*, 2546−2552.
(46) Ferrandez, A., Prescott, S., and Burt, R. (2003) COX-2 and colorectal cancer. *Curr. Pharm. Des. 9* (27), 2229−2251.
(47) Liu, B., Qu, L., and Yan, S. (2015) Cyclooxygenase-2 promotes tumor growth and suppresses tumor immunity. *Cancer Cell Int. 15*, 106.
(48) Xiong, B., Sun, T.-J., Yuan, H.-Y., Hu, M. B., Hu, W. D., and Cheng, F. L. (2003) Cyclooxygenase-2 expression and angiogenesis in colorectal cancer. *World J. Gastroenterol. 9*, 1237−1240.
(49) Elzagheid, A., Emaetig, F., Alkikhia, L., Buhmeida, A., Syrjänen, K., El-Faitori, O., Latto, M., Collan, M., and Pyrhönen, S. (2013) High cyclooxygenase-2 expression is associated with advanced stages in colorectal cancer. *Anticancer Res. 33*, 3137−3143.
(50) Jaiswal, P. K., Goel, A., and Mittal, R. D. (2015) Survivin: A molecular biomarker in cancer. *Indian J. Med. Res. 141* (4), 389−397.
(51) Groner, B., and Weiss, A. (2014) Targeting survivin in cancer: novel drug development approaches. *BioDrugs 28* (1), 27−39.
(52) Soleimanpour, E., and Babaei, E. (2015) Survivin as a Potential Target for Cancer Therapy. Asian Pac. *J. Cancer Prev. 16* (15), 6187−6191.
(53) Venugopal, A., and Uma Maheswari, T. (2016) Expression of matrix metalloproteinase-9 in oral potentially malignant disorders: A systematic review. *J. Oral Maxillofac. Pathol. 20* (3), 474−479.
(54) Patel, B. P., Shah, S. V., Shukla, S. N., Shah, P. M., and Patel, P. S. (2007) Clinical significance of MMP-2 and MMP-9 in patients with oral cancer. *Head Neck. 29* (6), 564−572.
(55) Lotfi, A., Mohammadi, G., Tavassoli, A., Mousaviagdas, M., Chavoshi, H., and Saniee, L. (2015) Serum levels of MMP9 and MMP2 in patients with oral squamous cell carcinoma. Asian Pac. *J. Cancer Prev. 16* (4), 1327−1330.
(56) Shpitzer, T., Hamzany, Y., Bahar, G., Feinmesser, R., Savulescu, D., Borovoi, I., Gavish, M., and Nagler, R. M. (2009) Salivary analysis of oral cancer biomarkers. *Br. J. Cancer 101* (7), 1194−1198.
(57) Chatterjee, S., Behnam Azad, B., and Nimmagadda, S. (2014) The intricate role of CXCR4 in Cancer. *Adv. Cancer Res. 124*, 31−82.
(58) Youle, R. J., and Strasser, A. (2008) The BCL-2 protein family: opposing activities that mediate cell death. *Nat. Rev. Mol. Cell Biol. 9*, 47−59.

(59) Frenzel, A., Grespi, F., Chmelewskij, W., and Villunger, A. (2009) Bcl2 family proteins in carcinogenesis and the treatment of cancer. Apoptosis: an. *Apoptosis 14* (4), 584−596.
(60) Sherin, D.R., Geethu, C.K., Prabhakaran, J., Mann, J. J., Dileep Kumar, J.S., and Manojkumar, T.K. (2019) Molecular docking, dynamics simulations and 3D-QSAR modeling of arylpiperazine derivatives of 3,5-dioxo-(2H,4H)-1,2,4-triazine as 5-HT1AR agonists. *Comput. Biol. Chem. 78*, 108−115.
(61) Schrödinger, LLC. (2020) *Schrödinger*, release 2020−1, Schrödinger, LLC, New York.
(62) RCSB Protein Data Bank. www.rcsb.org.

https://dx.doi.org/10.1021/acsptsci.1c00011
ACS Pharmacol. Transl. Sci. 2021, 4, 834−847